Journal of Applied Polymer Science

Fabrication of PLA/PEG/MWCNT Electrospun Nanofibrous Scaffolds for Anticancer Drug Delivery

Nadia Aboutalebi Anaraki,[1] Leila Roshanfekr Rad,[2] Mohammad Irani,[2,3] Ismaeil Haririan[2,4]

[1]Department of Chemical and Petroleum Engineering, Sharif University of Technology, Tehran, Iran
[2]Medical Biomaterials Research Center (MBRC), Tehran University of Medical Science, Tehran, Iran
[3]Department of Chemical Engineering, Amirkabir University of Technology (Tehran Polytechnic), Tehran, Iran
[4]Department of Pharmaceutics, School of Pharmacy, Tehran University of Medical Sciences, Tehran, Iran
Correspondence to: M. Irani (E-mail: iranimo@ut.ac.ir) and I. Haririan (E-mail: haririan@tums.ac.ir)

ABSTRACT: In the present study, polylactic acid (PLA)/polyethylene glycol (PEG)/multiwalled carbon nanotube (MWCNT) electrospun nanofibrous scaffolds were prepared via electrospinning process and their applications for the anticancer drug delivery system were investigated. A response surface methodology based on Box–Behnken design (BBD) was used to evaluate the effect of key parameters of electrospinning process including solution concentration, feeding rate, tip–collector distance (TCD) and applied voltage on the morphology of PLA/PEG/MWCNT nanofibrous scaffolds. In optimum conditions (concentration of 8.15%, feeding rate of 0.2 mL/h, voltage of 18.50 kV and TCD of 13.0 cm), the minimum experimental fiber diameter was found to be 225 nm which was in good agreement with the predicted value by the BBD analysis (228 nm). *In vitro* drug release study of doxorubicin (DOX)-loaded nanofibrous scaffolds, higher drug content induced an extended release of drug. Also, drug release rate was not dependent on drug/polymer ratio in different electrospun nanofibrous formulations. The equation of $M_t = c_0 + kt^{0.5}$was used to describe the kinetic data of DOX release from electrospun nanofibers. The cell viability of DOX-loaded nanofibrous scaffolds was evaluated using 3-(4,5-dimethylthiazol-2-yl)-2,5-diphenyltetrazolium bromide, a tetrazole assay on lung cancer A549 cell lines. We propose that DOX-incorporated PLA/PEG/MWCNT nanofibrous scaffold could be used as a superior candidate for antitumor drug delivery. © 2014 Wiley Periodicals, Inc. J. Appl. Polym. Sci. **2015**, *132*, 41286.

KEYWORDS: drug delivery systems; electrospinning; fibers

Received 29 March 2014; accepted 8 July 2014
DOI: 10.1002/app.41286

INTRODUCTION

The principle of ideal drug delivery system design involves targeted delivery with controlled release where drug is released in a certain and discriminatory fashion. The aim of all controlled release systems is to improve the efficacy of the drug and to reduce the systemic toxicity. Nowadays, most anticancer drugs have poor selectivity and high toxicity. Recently, there has been a wide attention in the development of novel drug delivery systems to improve the effectiveness of chemotherapy and reduce toxic side effects of anticancer drugs.[1,2] Many nanostructured drug delivery systems, such as polymeric micelles, polymeric nanofibers, nanoparticles, and liposomes have been studied to design an efficient drug delivery system.[3,4] In comparison to other nanostructured delivery systems, nanofibrous polymers have many advantages, including intrinsic high specific surface area, interfiber porosity, low hindrance for mass transfer, easy handling, and good mechanical strength.[4]

Many kinds of copolymers and polymer mixtures, such as poly(lactide-*co*-glycolide), poly(ethylene-*co*-vinyl alcohol), collagen/elastin, chitosan/poly(ethylene oxide) (PEO or PEG when) have been electrospun to fabricate nanofibrous scaffolds for biomedical applications such as drug delivery and tissue engineering.[5–9] Polylactic acid (PLA) is a biodegradable and biocompatible synthetic polymer that has been widely used in various biomedical applications. In addition, a wide variety of materials, such as polyethylene glycol (PEG), polyvinyl alcohol (PVA) and chitosan have been incorporated in the electrospun PLA nanofibrous scaffolds to tailor the fiber for particular end uses.[10] Furthermore, inorganic nanoparticles, such as $CaCO_3$,[11] Fe_3O_4,[12] and carbon nanotubes[13–15] have been incorporated into the fibers to release the drug in a controlled manner. When compared with other nanomaterials,[11–15] carbon nanotubes (CNTs) have unique structures including high aspect ratios, high surface areas, and nanosized stable tubes.[16–18] Multiwalled carbon nanotubes (MWCNTs), due to their extraordinary properties such as excellent mechanical, electrical and thermal properties, is one of the most promising candidates for design of novel composite scaffold by introducing small amounts of MWCNTs into the polymer.[19]

© 2014 Wiley Periodicals, Inc.

In the fabrication of nanofibers prepared by electrospinning process, several parameters such as polymer concentration, feeding rate, voltage, and tip–collector distance (TCD) influence on the diameter and morphology of fibers.[10] In the electrospinning process, it is very important to obtain nanofibers with minimum diameter; because the thinner and homogeneous fibers provide the maximum surface area and porosity, which is an advantage for the higher loading of drug onto the nanofibrous scaffolds. Investigation of each factor separately on the morphology of fibers would be very time consuming. Therefore, statistical experimental design methods could be used to evaluate the effect of variables and optimization of experimental parameters. Response surface methodology is essentially a particular set of mathematical and statistical methods for experimental design and evaluating the effects of variables and searching optimum conditions of variables.[20] In recent researches, the factor space central-composite design (CCD) and Box–Behnken design (BBD) are commonly selected experimental design techniques.[20,21]

In the present work, a sustained release anticancer drug delivery systems, using electrospun poly(lactic acid) nanofibrous scaffolds have been studied. BBD was used to investigate the effects of feeding rate, solution concentration, voltage, and distance and optimization of parameters on the electrospun nanofibers to obtain controllable diameter of these nanofibers. To investigate the utility of these biocompatible polymeric scaffolds for long-term delivery of anticancer drugs, DOX-loaded nanofibrous scaffolds were prepared via electrospinning method. *In vitro* release profile and antitumor activity of the DOX-containing fibers were investigated. The effect of PEG- and CNT-loaded PLA nanofibers on the release behavior were also evaluated.

EXPERIMENTAL

Materials

Polylactic acid ($M_w = 186{,}000$), phosphate buffered saline (PBS), and polyethylene glycol ($M_w = 4000$) were provided by Sigma-Aldrich Chemie Gmbh. *N,N*-dimethyl formamide (DMF), chloroform, and acetone were purchased from Merck & Co. Multiwall carbon nanotubes were prepared from nanobiomedical laboratory (Tehran, Iran). The obtained MWCNTs have average diameters of 30–70 nm and length of 1–2 μm. Doxorubicin was purchased from Sobhan Pharmaceuticals.

Preparation of Electrospun Solutions

Adequate 10% (w/v) of PLA was dissolved in a solvent mixture of acetone and chloroform in the ratio of 9:1 by stirring at 55°C. Then different amounts of PEG (10, 20, and 30% mass of PEG to PLA) were added—to the PLA solution.

For preparation of PLA/PEG/MWCNT, first, MWCNTs were dispersed in *N,N*-dimethyl formamide (DMF) (good solvent for PLA and MWCNTs dispersion) at different concentrations with ultrasonication for 2 h and then stirred continuously overnight at room temperature. After that the various MWCNTs contents (0.5, 1, 2, and 5%, mass of MWCNTs to PLA) were slowly dispersed to the PLA/PEG solution drop by drop at room temperature and were sonicated for extra 2 h and finally, were stirred continuously for 24 h before electrospinning.

Electrospinning

The prepared solution was loaded into a 5 mL plastic syringe attached to a syringe needle (inner diameter of 0.4 mm). This was placed to a KD programmable syringe pump (Nanomeghyas company) to control the solution flow rate. The applied voltage was in the range of 15–20 kV. The feeding rate was adjusted in the range 0.2–1 mL/h and TCD was varied in the range of 10–15 cm. The electrospun nanofibers were collected on a metal drum (9 cm diameter) as an electrode, rotating at approximately 1000 rpm. The prepared nanofiber scaffolds were vacuum dried at room temperature for three days to completely remove any solvent residue prior to the experiments. The set up of electrospinning process was provided by Nanomeghyas company (Nanomeghyas, Iran).

Design of Electrospinning Process

In the current study, four-factor three-level BBD was used to determine the relation between electrospinning parameters containing the solution concentration, applied voltage, feeding rate and TCD on the PLA/PEG/MWCNT nanofiber diameter. All experiments were repeated three times and the results were given as averages. The results of the experimental design were studied using MINITAB 16 statistical software to estimate the response of the dependent variable.

The BBD response surface model of electrospinning experiments expresses the diameter of PLA/PEG/MWCNT nanofibers (nm) as a function of the above mentioned parameters. The polynomial model for diameter of nanofibers (nm) with respect to the electrospinning parameters is expressed as follows:

$$\text{Diameter of fiber} = \beta_0 + \sum_{i=1}^{3} \beta_i x_i^2 + \sum_{i=1}^{3} \beta_{ii} x_i^2 + \sum_{i=1}^{3} \sum_{j=1}^{3} \beta_{ij} x_i x_j \quad (1)$$

where β_0, β_i, β_{ii}, β_{ij} are the constant regression coefficient of the model and x_i, x_{ii}, and x_{ij} represent the linear, quadratic, and interactive terms of the uncoded independent variables, respectively. The experimental design and results of fiber diameter are shown in Table I.

Scanning Electron Microscopy (SEM)

Morphological studies of prepared nanofibers were carried out using a scanning electron microscope (SEM, JEOL JSM-6380). Electrospun nanofibers collected on the aluminum foil were cut into pieces of 1×1 cm^2. Samples were coated with a thin layer of gold by a Bio-Rad E5200 auto sputter coater at an accelerating voltage of 10 kV for 5 min. The average diameter of nanofibers was obtained with an image analyzer (Image-Proplus, Media Cybernetics). From each image, at least 100 different fiber segments were randomly selected and their diameters measured to generate an average fiber diameter.

Drug Incorporation and Loading Efficiency

The anticancer DOX was incorporated into the composite solution prior to electrospinning to produce a solution of both polymer and DOX. DOX was used at loading percentages of 10, 20, and 50% of the initial polymer weight. For preparation of homogeneous solutions, the solutions were emulsified at a

Table I. The Experimental Design and Results of Fiber Diameter Versus Independent Variables Used in Electrospinning Process

Run order	Concentration (%) (X_1)	Feeding rate (mL/h) (X_2)	Voltage (kV) (X_3)	Distance (cm) (X_4)	Nanofiber diameter (nm)	Fitted value by model (nm)
1	6	0.2	17.5	12.5	260	259
2	10	0.2	17.5	12.5	255	254
3	6	1.0	17.5	12.5	290	289
4	10	1.0	17.5	12.5	283	283
5	8	0.6	15.0	10.0	295	294
6	8	0.6	20.0	10.0	275	275
7	8	0.6	15.0	15.0	278	276
8	8	0.6	20.0	15.0	255	254
9	6	0.6	17.5	10.0	305	304
10	10	0.6	17.5	10.0	300	299
11	6	0.6	17.5	15.0	285	285
12	10	0.6	17.5	15.0	280	280
13	8	0.2	15.0	12.5	250	250
14	8	1.0	15.0	12.5	280	280
15	8	0.2	20.0	12.5	230	229
16	8	1.0	20.0	12.5	260	259
17	6	0.6	15.0	12.5	285	285
18	10	0.6	15.0	12.5	280	280
19	6	0.6	20.0	12.5	265	264
20	10	0.6	20.0	12.5	260	259
21	8	0.2	17.5	10.0	270	269
22	8	1.0	17.5	10.0	300	299
23	8	0.2	17.5	15.0	250	250
24	8	1.0	17.5	15.0	280	280
25	8	0.6	17.5	12.5	255	255
26	8	0.6	17.5	12.5	255	255
27	8	0.6	17.5	12.5	255	255

rotating rate of around 6500 r/min for about 1 h before electrospinning process. Then, the homogeneous mixed drug/polymer solutions with different DOX concentrations were electrospun in optimum conditions of electrospinning process. The amount of DOX loading nanofibrous scaffold was determined at the absorbance of 483.5 nm using UV–vis spectrophotometer.

$$\text{Drug content}\,(\%) = [\text{drug weight in the nanofiber} / \text{weight of the nanofiber}] \times 100\% \quad (2)$$

$$\text{Loading efficiency}\,(\%) = [\text{residual drug in the nanofiber} / \text{initial feeding amount of the drug}] \times 100\% \quad (3)$$

In Vitro Drug Release Study

The *in vitro* release profiles of DOX from nanofibrous scaffolds were investigated in phosphate buffer solution (pH 7.4). The amount of released DOX in the buffer solution was monitored by a UV–vis spectrophotometer at the wavelength of 483.5 nm. The drug-loaded fiber sample (50 mg) was incubated at 37°C in 20 mL of 0.05 M phosphate buffered saline (PBS, pH 7.4). The suspensions were placed in a shaking water bath (Hidolff) that was maintained at 37°C and 100 rpm of stirring for 60 days. Samples of 2.0 mL released solution were taken from the dissolution medium at predetermined intervals (1, 2, 3, 6, 12, 24, 48, 72, 120, 168, 240, 360, 480, 600, 720, 1080, and 1440 h) while equal amount of fresh buffer solutions was added back to the incubation media. The amount of DOX present in release buffer was determined by converting of its detected UV absorbance to its concentration according to the calibration curve of known concentrations of DOX in the same buffer.

Cell Viability Test

Cell viability test was determined using a colorimetric 3-(4,5-dimethylthiazol-2-yl)-2,5-diphenyltetrazolium bromide, a tetrazole (MTT) assay as previously described.[22] Briefly, the cells were cultured at 37°C in a humidified atmosphere containing 5% CO_2, dissociated with 0.25% trypsin in PBS (pH 7.4) and centrifuged at 1000 rpm for 7 min at room temperature (TD5A pharmacy centrifuge). Then 30,000–40,000 cells were cultured in each well of 96-well plates and after 24 h time periods, to allow attachment of the cell to the wells, different concentrations of the materials were treated to the cells. In this context,

Table II. Analysis of Variance (ANOVA) Results for Experimental Response at Different Factor Levels

Source	DF	Seq SS	Adj MS	*F*	*P*
Regression	14	8925.21	637.52	1732.12	0.000
Linear	4	5127.17	469.70	1276.17	0.000
X_1	1	85.33	625.56	1699.63	0.000
X_2	1	2640.33	12.92	35.10	0.000
X_3	1	1260.75	2.62	7.11	0.021
X_4	1	1140.75	1211.77	3292.37	0.000
Square	4	3794.80	948.70	2577.60	0.000
X_1^2	1	1149.90	1579.34	4291.04	0.000
X_2^2	1	190.68	0.45	1.23	0.289
X_3^2	1	249.19	0.59	1.61	0.229
X_4^2	1	2205.04	2205.04	5991.04	0.000
Interaction	6	3.25	0.54	1.47	0.267
X_1 X_2	1	1.00	1.00	2.72	0.125
X_1 X_3	1	0.00	0.00	0.00	1.000
X_1 X_4	1	0.00	0.00	0.00	1.000
X_2 X_3	1	0.00	0.00	0.00	1.000
X_2 X_4	1	0.00	0.00	0.00	1.000
X_3 X_4	1	2.25	2.25	6.11	0.029
Residual error	12	4.42	0.37		
Lack-of-fit	10	4.42	0.44	0.44	0.44
Pure error	2	0.00	0.00		
Total	26	8929.63			

different concentrations of nanofibers, DOX-loaded nanofibers and free DOX were prepared with 1% DMSO and treated to the cells at different time periods. However, media containing 1% DMSO was used as negative control. The MTT assay was as follows: 20 μL of MTT solution (5 mg/mL) in PBS (pH 7.4) was added to each well. The incubation was continued for another 4 h and then the solution was aspirated cautiously from each well. After treating the cells with Sorenson buffer, the optical density of each well was read using a microplate reader (Multiskan MK3, Thermo Electron Corporation) at a wavelength of 570 nm, and growth inhibition was calculated.

RESULTS AND DISCUSSION

Design of Experiment for Fabrication of PLA Nanofiber

Analysis of Experimental Design. Four factors of electrospinning process including PLA/PEG/MWCNT concentration, feeding rate, applied voltage and TCD at three levels were investigated for fabrication of PLA/PEG/MWCNT fibers. Analysis of variance (ANOVA) was performed to evaluate a full quadratic response surface model. *P* value is a measure of statistical significance and the electrospinning parameter that shows significant impact on the average fiber diameter would have *P* value is less than 0.05 at 95% confidence interval. Table II, revealed those linear terms, two quadratic terms (X_1^2, and X_4^2) and one of the interaction terms (X_3X_4) exhibited significant effect on the fiber diameter.

By elimination of insignificant terms ($P > 0.05$) from the full quadratic model, eq. (4) which includes a series of linear, quadratic and interaction terms for the four electrospinning variables was designed, as follows:

$$\text{Diameter of fiber (nm)} = 1120.93 - 70.12X_1 + 37.08X_2 - 2.60X_3 - 83.09X_4 + 4.3{X_1}^2 + 3.25{X_4}^2 - 0.12X_3X_4 \quad (4)$$

The goodness-of-fit measure of the model was evaluated using the coefficient of determination (R^2). The high value of ($R^2 = 0.986$) indicated a high reliability of the model in predicting the diameter of PLA nanofiber.

3D Surface and Counter Plots. The three-dimensional response surface plots are depicted in Figure 1. As shown in Figure 1(a), varying the voltage and distance at the time was very important in the formation of electrospun nanofibers. This conclusion was also supported by the ANOVA table, which indicated that the interaction term between the applied voltage and distance was significant. At the voltage lower than 17.5 kV, the electrical force was not enough to form the homogenous fibers. When the voltage was increased to 17.5, the uniform thinner fibers were obtained. At the higher voltage values, the strength of the electrical field was high which resulted in higher instabilities of jet solution and fibers with larger diameter were formed on the collector. Similar trends are reported by other researchers.[23–25] In very short distance (10 cm), the electrical field became very strong which caused the jet of spinning solution to become unstable and bead fibers were obtained. When the needle TCD increased to 12.5 cm, the uniform fibers with the smaller

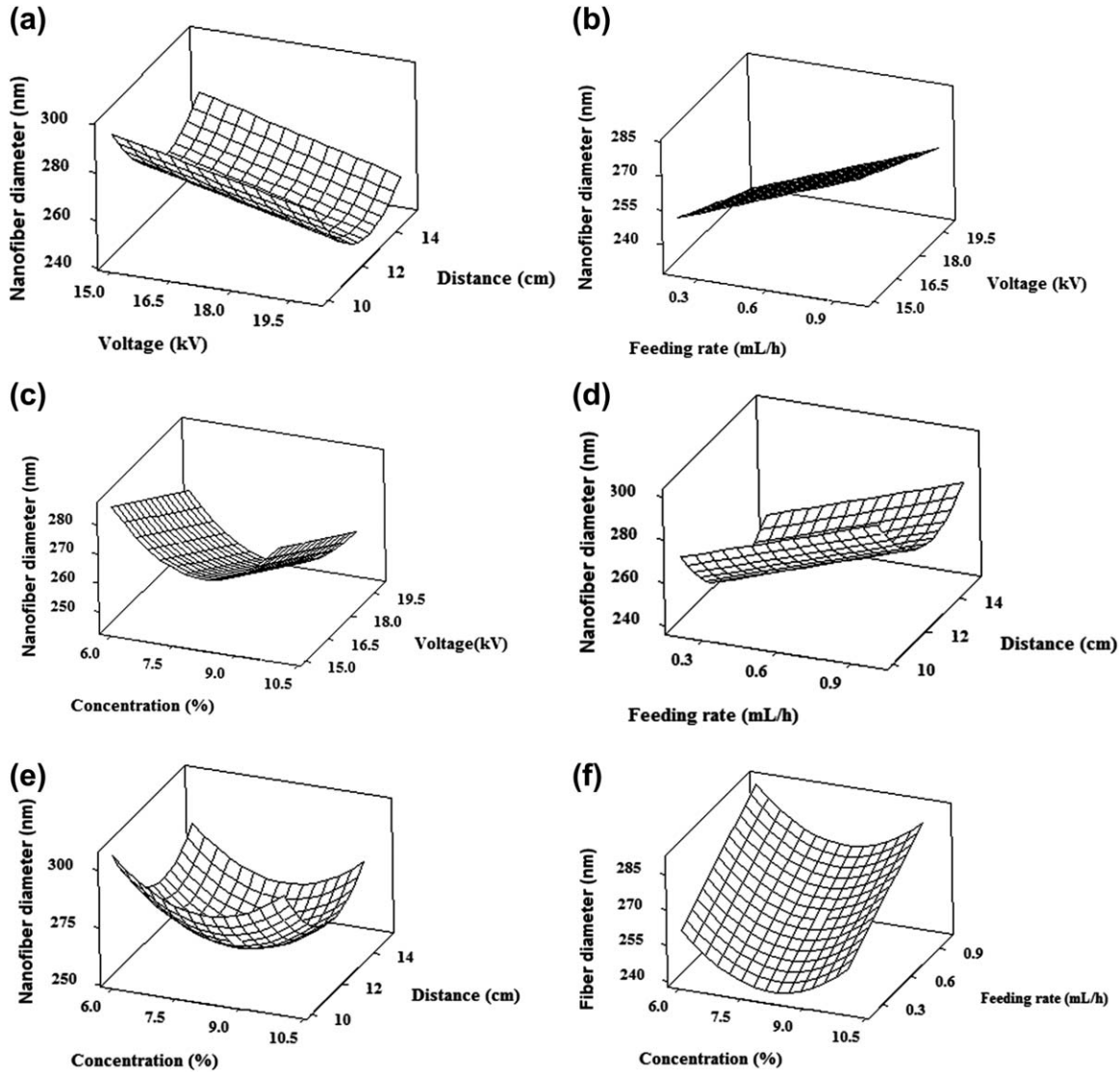

Figure 1. Surface plots of the response variable (fiber diameter, nm) for the different experimental factors (two factor at a time). (a) Distance and applied voltage, (b) feeding rate and voltage, (c) solution concentration and voltage, (d) feeding rate and distance, (e) solution concentration and distance, and (f) feeding rate and solution concentration.

diameters were formed (figure is not shown).[26] At the higher distance values, the strength of electrical force on the spinning solution was decreased which resulted in the formation of fiber with larger diameters.[26,27] The surface plots for applied voltage versus flow rate and voltage versus concentration indicated that the adjusted amount of applied voltage produced the thinner fibers [Figure 1(b,c)]. Also, it was observed that varying of distance played a fundamental role in the fiber diameter at different solution feeding rates and solution concentrations [Figure 1(d,e)]. Figure 1(f) shows the surface plot of average fiber diameter (nm) as a function of feeding rate and solution concentration. As shown, the lower feeding rate (0.2 mL/h) in the middle amounts of solution concentration (8%) led to produce the homogeneous and fine fibers. By increasing the solution feeding rate, the electrostatic density of solution was decreased which led to produce the bigger fibers as compared to lower flow rates.[28,29]

Optimization of Nanofiber Diameter. By solving eq. (4), the optimal uncoded values of applied voltage, feeding rate, TCD, and solution concentration were estimated to be 18.5 kV, 0.2 mL/h, 13 cm, and 8.15%, respectively. Thus, the minimum fiber diameter of PLA/PEG/MWCNT nanofiber was found to be 228 ± 25 nm. For identical electrospinning parameters, the experimental average nanofiber diameter value for three replicates was obtained as 225 nm, which was very close to the predicted value by the response model.

Validation of the Experimental and Predicted Model Data. The experimental average diameter of nanofiber was compared with the predicted values of the response model [Figure 2(a)]. As shown, the experimental values of nanofiber diameter were in close agreement with the predicted values of model. The probability distribution plot of residuals (difference between the model predicted fiber diameter values and

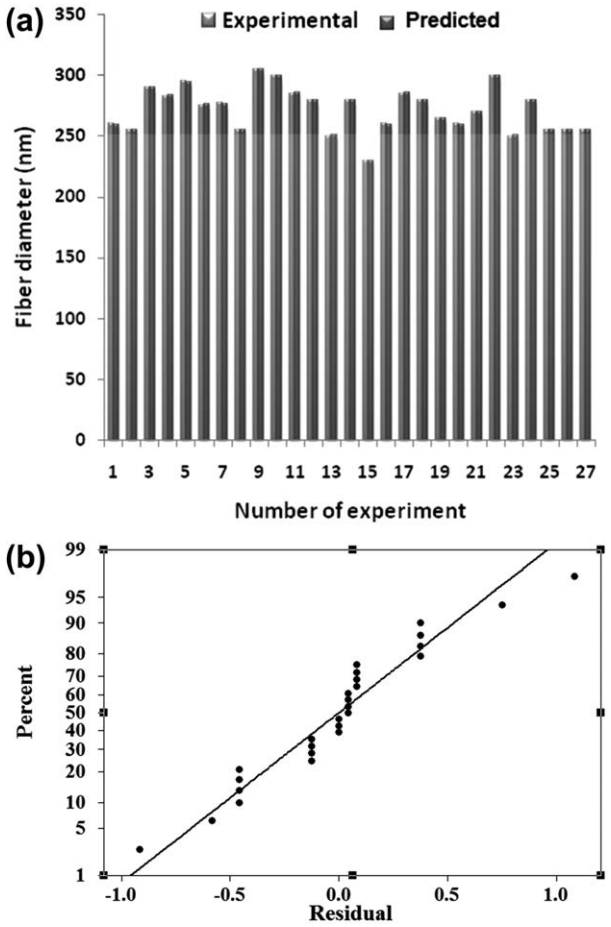

Figure 2. (a) Plot of model predicted fiber diameter against experimental fiber diameter (eq. 4) and (b) normal probability plot.

those derived experimentally) are presented in Figure 2(b). The errors were normally distributed, as all the points were close to the line.[30] Furthermore, it was observed that the established model was sufficient to estimate the average diameter of PLA/PEG/MWCNT nanofiber, as all the residuals were smaller than 5%.

SEM Images of Electrospun Nanofiber Scaffolds

The SEM images of PLA/PEG/MWCNT nanofibers are typically shown in Figure 3 (experiment number of 7 at solution concentration of 8%, feeding rate of 0.6 mL/h, voltage of 15 kV, and distance of 15 cm and experiment number of 27 at solution concentration of 8%, feeding rate of 0.6 mL/h, voltage of 17.5 kV, and distance of 12.5 cm). As shown, when the applied voltage and TCD were 15 kV and 15 cm, the bead fibers were produced [Figure 3(a)]. Whereas increase in voltage to 17.5 kV and decrease in TCD to 12.5 cm resulted in the fabrication of fine and homogeneous fibers [Figure 3(b)]. Therefore, varying the applied voltage and distance between needle tip and collector was very important to spin thinner fibers. Also, the SEM image of nanofibrous scaffold after optimization of electrospinning process is shown in [Figure 3(c)]. As can be seen, by optimizing the parameters, the thinner fibers with sharp diameter distribution in comparison to fibers before optimization were formed.

The SEM image of the electrospun DOX-loaded PLA/PEG/MWCNT nanofibrous scaffold (typically 20 wt % of DOX loading) is shown in Figure 3(d). As shown, no drug crystals were identified on the surface of nanofibers. It can be due to the adsorption of DOX onto the sidewalls of MWCNT. Similar trends are reported by other researches.[31,32]

Drug Content and Loading Efficiency

The drug content and loading efficiency of DOX loaded PLA/PEG/MWCNT nanofibrous scaffolds were evaluated. Based on results, the drug contents of 10, 20, and 50% samples (drug/polymer solution, weight ratio) were found to be 9.8 ± 0.1, 19.2 ± 0.3, and $47.7 \pm 1\%$ (w/w), respectively. The loading efficiency of prepared scaffolds was obtained as 94 ± 2, 92 ± 3, and $87 \pm 3\%$ (w/w), respectively. These results indicated that DOX may be finely incorporated into the nanofibrous scaffolds.

In Vitro Drug Release

The release profiles of DOX-loaded PLA, PLA/PEG, and PLA/PEG/MWCNT nanofibrous scaffolds are shown in Figure 4. As shown, the release profiles of DOX from nanofibers were characterized by two stages: (a) a rapid release stage (the first 24 h) and (b) a slow release stage (from 24 to 720 h). Initial burst release of DOX fibers within first hours was mainly due to the diffusion of DOX dispersing close to the surface of polymer fibers, which diffused out quickly in initial incubation times. The pores left after initial burst release and subsequent drug diffusion were critical for further release from the inner sections of fibers through the swollen and porous inner structure. Therefore, the equation of $M_t = c_0 + kt^{0.5}$ was used to describe the kinetic data of DOX release from electrospun nanofibers ($R^2 > 0.985$ for all equations obtained from data plotting of percent of drug released versus time). First parameter was related to the initial burst release and second parameter was attributed to the diffusion of drug through the pores of nanofibers. Furthermore, the statistical comparison among slope of release equations showed no significant differences ($P > 0.05$) which indicated that the drug release rate was not dependent on drug/polymer ratio in different formulations.

Comparison of DOX loaded PLA, PLA/PEG, and PLA/PEG/MWCNT nanofibrous scaffolds revealed that the release percentages of DOX loaded PLA nanofibrous scaffolds with different concentrations of DOX were the lowest. Their release percentages were about 21, 15.5, and 10.5% after 24 h and about 37.5, 27, and 17.5% after 30 days for 10, 20, and 50% DOX-loaded nanofibrous scaffolds. Furthermore, the release percentages of DOX from the PLA/PEG nanofibers were enhanced by increasing the PEG /PLA ratios. As the PEG is more soluble in water, the increasing of PEG percentages in nanofibrous formulations may have caused DOX to migrate towards the outside of nanofibrous scaffolds. In contrast, the release behavior of DOX from PLA/PEG/MWCNT nanofibrous scaffold was the slowest. In the case of loading drugs such as DOX onto the side walls of MWCNTs via π-stacking interaction, it was realized by simply mixing DOX and MWCNTs in aqueous solution, thus allowing DOX to be adsorbed onto the side walls of MWCNTs. By varying of PEG/MWCNT ratios could be fine tuned to specific release rates. Therefore, the PLA/PEG/MWCNT due to the

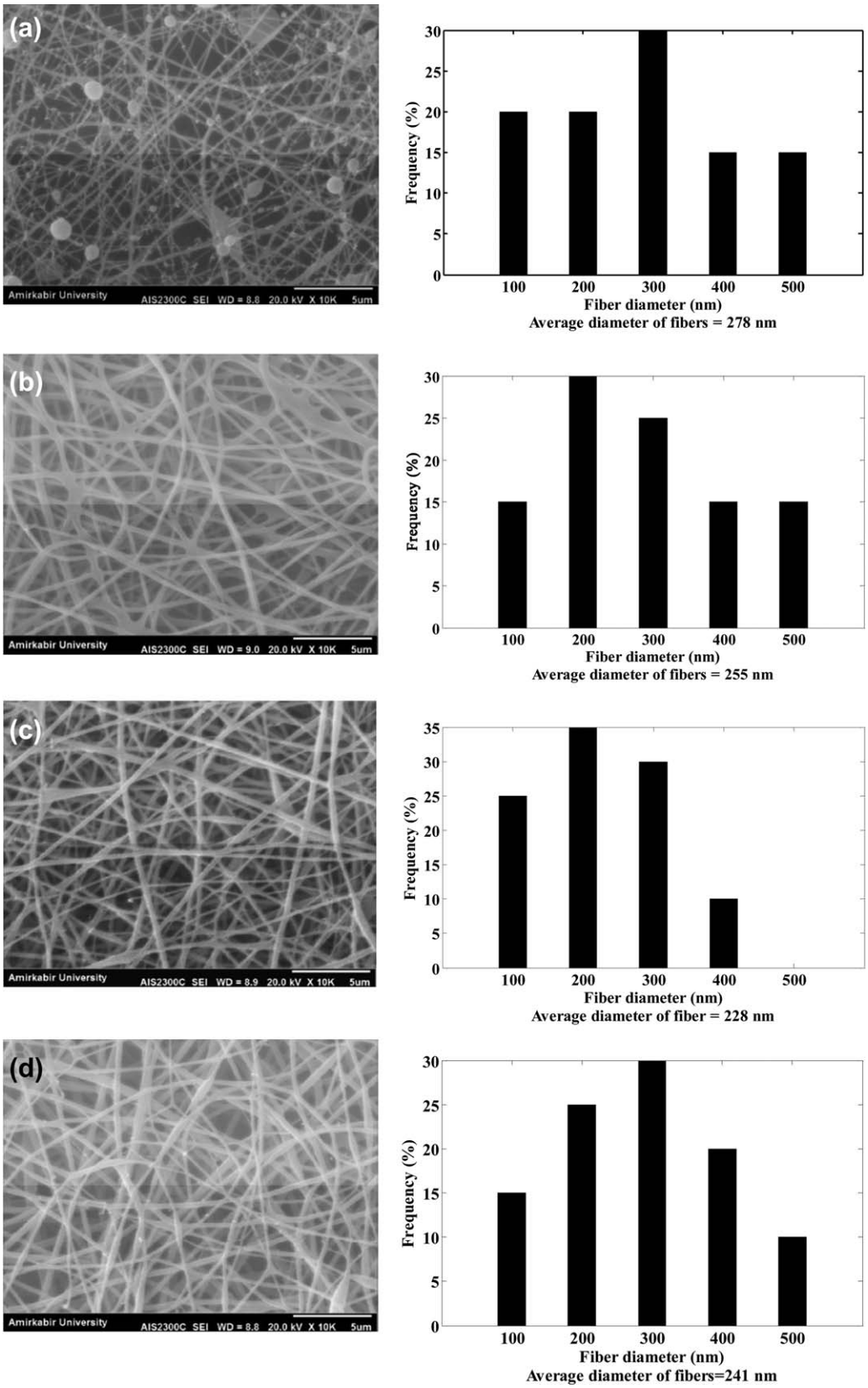

Figure 3. SEM images of PLA/PEG/MWCNT nanofibers at different electrospinning conditions (a) concentration of 8%, feeding rate of 0.6 mL/h, voltage of 15 kV and distance of 15.0 cm, (b) concentration of 8%, feeding rate of 0.6 mL/h, voltage of 17.50 kV and distance of 12.5 cm, (c) concentration of 8.15%, feeding rate of 0.2 mL/h, voltage of 18.50 kV and distance of 13.0 cm, and (d) DOX 20%-loaded PLA/PEG 20%/CNT 2% nanofibrous scaffolds.

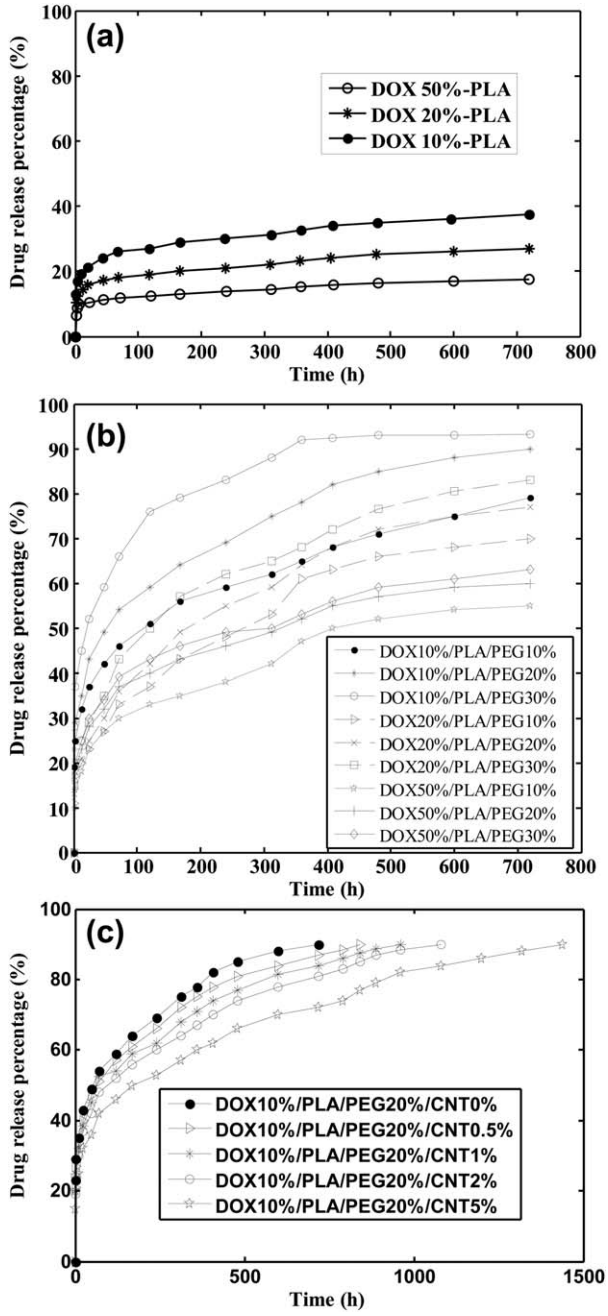

Figure 4. The release behavior of the DOX loaded (a) PLA, (b) PLA/PEG, and (c) PLA/PEG/MWCNT nanofibrous scaffolds.

higher DOX release and slower release behavior would be an ideal choice for cancer therapy.

In Vitro Cell Viability

Cell viability of the various samples including free DOX, DOX-loaded PLA/PEG/MWCNT fibers, and the pure PLA/PEG/MWCNT fibers without drug after 72 h incubation is shown in Figure 5.

It implied that the DOX-loaded PLA/PEG/MWCNT fibers exhibited obvious cytotoxicity against A549 cells more longer time than free DOX due to its capacity of sustained released time. Moreover, the DOX was released from nanofibers without losing cytotoxicity during a long time period (48–72 h) seems to be more potent than free DOX with 16–18 h half life.[33] In the case of blank nanofibers without DOX, the sample did not display any cytotoxicity to A549 cells compared with the control up to 72 h. However, 72 h treatment of the cells with 0.2–1 mg/mL DOX-loaded PLA/PEG/MWCNT nanofibers obtained nearly 65–92% cells death, respectively, that is very high compared with free DOX (60–62%), yet the control nanofibrous scaffold showed nontoxic properties. The results indicated that DOX loaded PLA/PEG/MWCNT nanofiber scaffold could be used as an alternative source of free DOX due to its capacity to release over a long time from the PLA/PEG/MWCNT nanofibrous scaffold without losing its anticancer capability.

CONCLUSION

In this study, PLA/PEG/MWCNT nanofibrous scaffold were fabricated by electrospinning technique. Doxorubicin hydrochloride (DOX), an anticancer drug, was successfully encapsulated into these nanofibrous scaffolds. The response surface methodology based on BBD was used to determine the relation of electrospinning process parameters on the diameter of electrospun nanofibers. Four factors of electrospinning process including, solution concentration, voltage, TCD and feeding rate of solution were evaluated at three levels in fabrication of electrosun nanofibers. By optimizing the process parameters (applied voltage of 18.5 kV, feeding rate of 0.2 mL/h, TCD of 13 cm and PLA concentration of 8.15%), the minimum diameter of PLA nanofibers was estimated to be 228 nm. This datum was in a good match with the experimental datum of fiber diameter (225 nm). DOX was finely incorporated in the fibers and no DOX crystals were detected on the fiber surfaces. The release rate of DOX from the fibers was dependent on the initial DOX loading. During the whole release time, the rate of DOX release decreased as the DOX content in the fibers increased. The sustained released could last for more than 30 days. The cell viability of DOX loaded nanofibers exhibited superior cytotoxic activities of DOX loaded PLA/PEG/MWCNT nanofibrous scaffolds.

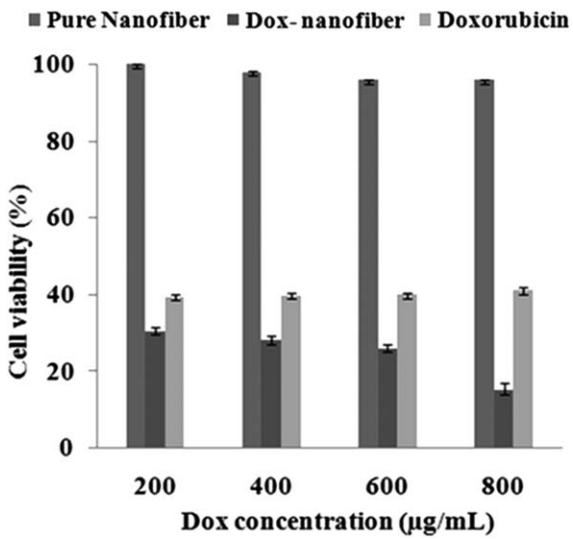

Figure 5. Cell viability of A549 cells, at different DOX, free nanofiber, and DOX-loaded nanofibers.

REFERENCES

1. Ahmed, N.; Fessi, H.; Elaissari, A. *Drug Discov. Today* **2012**. doi:10.1016/j.drudis.2012.03.010.
2. Vandghanooni, S.; Eskandani, M. *Bio Impacts* **2011**, *1*, 87.
3. Yoo, H. S.; Park, T. G. *J. Control Release* **2001**, *70*, 63.
4. Wang, Z. G.; Wan, L. S.; Liu, Z. M.; Huang, X. J.; Xu, Z. K. *J. Mol. Catal. B: Enzymol.* **2009**, *56*, 189.
5. Liang, D.; Hsiao, B. S.; Chu, B. *Adv. Drug Deliv. Rev.* **2007**, *59*, 1392.
6. Qi, R.; Guo, R.; Zheng, F.; Liu, H.; Yu, J.; Shi, X. *Colloid Surf. B: Bioint.* **2013**, *110*, 148.
7. Abdal-hay, A.; Sheikh, F. A.; Lim, J. K. *Colloid Surf. B: Bioint.* **2013**, *110*, 635.
8. Zong, X.; Kim, K.; Fang, D.; Ran, S.; Hsiao, B. S.; Chu, B. *Polymer* **2002**, *43*, 4403.
9. Luu, Y. K.; Kim, K.; Hsiao, B. S.; Chu, B.; Hadjiargyrou, M. *J. Control Release* **2003**, *89*, 341.
10. Efthimiadou, E. K.; Tziveleka, L. A.; Bilalis, P.; Kordas, G. *Int. J. Pharm.* **2012**, *428*, 134.
11. Fujihara, K.; Kotaki, M.; Ramakrishna, S. *Biomaterials* **2005**, *26*, 4139.
12. Lin, T. C.; Lin, F. H.; Lin, J. C. *Acta Biomater.* **2012**, *8*, 2704.
13. Shao, S.; Zhou, S.; Li, L.; Li, J.; Luo, C.; Wang, J.; Li, X.; Weng, J. *Biomaterials* **2011**, *32*, 2821.
14. Zong, X.; Kim, K.; Fang, D.; Ran, S.; Hsiao, B. S.; Chu, B. *Polymer* **2002**, *43*, 4403.
15. Luu, Y. K.; Kim, K.; Hsiao, B. S.; Chu, B.; Hadjiargyrou, M. *J. Control Release* **2003**, *89*, 341.
16. Kam, N.W.S.; O'Connell, M.; Wisdom, J. A.; Dai, H. J. *Proc. Natl. Acad. Sci.* **2005**, *102*, 11600.
17. Shao, N.; Lu, S.; Wickstrom, E.; Panchapakesan B. *Nanotechnology* **2007**, *18*, 101.
18. Zeineldin, R.; Al-Haik, M.; Hudson, G. *Nano Lett.* **2009**, *9*, 751.
19. Sung, J. H.; Kim, H. S.; Jin, H. J.; Choi, H. J. *J. Chin. Macromol.* **2004**, *37*, 9899.
20. Heikkilä, P.; Harlin, A. *Eur. Polym. J.* **2008**, *44*, 3067.
21. Myers, R. H.; Montgomery, D. C.; Anderson-Cook, C. M. Wiley: New York; **2009**.
22. Xu, X.; Yang, L.; Xu, X.; Wang, X.; Chen, X.; Liang, Q.; Zeng, J.; Jing. X. *J. Control Release* **2005**, *108*, 33.
23. Gu, S. Y.; Ren, J. *Macromol. Mater. Eng.* **2005**, *290*, 1097.
24. Lee, C. K.; Kim, S. I.; Kim, S. J. *Synth. Met.* **2005**, *154*, 209.
25. Irani, M.; Keshtkar, A. R.; Moosavian, M. A. *Chem. Eng. J.* **2012**, *200*, 192.
26. Subbiah, T.; Bhat, G. S.; Tock, R. W.; Parameswaran, S.; Ramkumar, S. S. *J. Appl. Polym. Sci.* **2005**, *96*, 557.
27. Zong, X. H.; Kim, K.; Fang, D. F.; Ran, S. F.; Hsiao, S. F.; Chu, X. B. *Polymer* **2002**, *43*, 4403.
28. Cui, W.; Li, X.; Zhou, S.; Weng, J. *J. Appl. Polym. Sci.* **2007**, *103*, 3105.
29. Park, Y.; Lee, I. H.; Bea, G. N. *J. Ind. Eng. Chem.* **2008**, *14*, 707.
30. Salehi, R.; Irani, M.; Rashidi, M.-R.; Aroujalian, A.; Raisi, A.; Eskandanic, M.; Haririan, I.; Davaran, S. *Des. Monom. Polym.* **2013**, *16*, 515.
31. Zhang, X.; Meng, L.; Lu, Q.; Fei, Z.; Dyson, P. *J. Biomater.* **2009**, *30*, 6041.
32. Tripisciano, C.; Kraemer, K.; Taylor, A.; Borowiak-Palen, E. *Chem. Phys. Lett.* **2009**, *478*, 200.
33. Laginha, K. M.; Verwoert, S.; Charrois, G. J.; Allen, T. M. *Clin. Cancer Res.* **2005**, *11*, 69449.